PFG 2012 / 1, 0029–0038
Stuttgart, January 2012

Article

SNR Evaluation of the RapidEye Space-borne Cameras

Ralf Reulke, DLR, Berlin & Horst Weichelt, RapidEye, Brandenburg

Keywords: SNR, in-flight noise determination, space camera assessment

Summary: After launch and during continuous radiation exposure, space-borne cameras are constantly changing. Therefore, permanent technical determination and evaluation of the sensor in space plays an important role in the remote sensing community. There are a variety of evaluation criteria, which are all based on the essential camera parameters – the spatial resolution, point spread function (PSF) and noise.

Noise estimation is a challenging task for characterization of remote sensing systems in space. The in-flight measurement of noise will often be done with artificial test sites. If these test sites are not sufficiently available, homogeneous image regions (desert, snow, water surfaces) are often used. The albedo of these regions, however, lies normally outside the specified albedo range of remote sensing systems focused on agriculture and forestry areas. The only possibility to determine the noise after the satellite launch within the specified operational albedo range is to use very small image areas with the required albedo within the acquired imagery. As these objects have to be homogeneous, one needs methods that can detect the smallest homogeneous areas in the image to evaluate noise.

In this paper an approach for determining the signal-to-noise ratio (SNR) with data from natural targets is presented. In experiments, the results demonstrate that the described method performs quite satisfactorily and results are comparable to the standard methods used to determine SNR.

Zusammenfassung: *SNR Bestimmung der RapidEye Weltraumkameras*. Durch den Start und die kontinuierliche Strahlenbelastung verändern sich Weltraumkameras laufend. Deshalb ist die ständige Spezifizierung und Bewertung solcher Sensoren von eminenter Bedeutung in der Fernerkundung. Es gibt eine Vielzahl von Bewertungskriterien, die auf den wesentlichen Parametern einer Kamera basieren – die räumliche Auflösung, die Punktbildverwaschungsfunktion (PSF) und das Rauschen.

Die quantitative Bestimmung des Rauschens aus Daten von Weltraumkameras ist eine anspruchsvolle Aufgabe. In-flight Messungen des Rauschens werden oft anhand künstlicher Testflächen durchgeführt. Wenn diese nicht ausreichend zur Verfügung stehen, verwendet man normalerweise homogene Bildbereiche (Wüste, Schnee, Wasseroberflächen). Diese sind jedoch außerhalb des Albedobereichs von interessanten Gebieten, die üblicherweise mittels Fernerkundungssystemen untersucht werden. Für das Fernerkundungssystem RapidEye sind das zum Beispiel landwirtschaftliche Gebiete und Forsten. Um das Rauschen nach dem Satellitenstart im spezifizierten operationellen Albedobereich zu bestimmen, ist es erforderlich, die Auswertung in diesen Bildregionen durchzuführen. Deshalb braucht man Methoden, die kleinste homogene Bereiche im Bild erkennen und bezüglich des Rauschens auswerten können.

In diesem Artikel wird ein Konzept für die Bestimmung des Signal-Rausch-Verhältnisses (SNR) aus Daten natürlicher Szenen vorgeschlagen. Untersuchungen zeigen, dass das Verfahren zufriedenstellend arbeitet und die Ergebnisse mit den konventionellen Verfahren vergleichbar sind.

1 Introduction

Calibration, verification and validation of remote sensing systems are the most challenging procedures after completion of the sensor.

Using the sensor calibration, radiometric and geometric correction of the image data is possible. At the same time, the relationship between gray values and radiance is established.

www.schweizerbart.de
DOI: 10.1127/1432-8364/2012/0100
1432-8364/12/0100 $ 2.50

The same data set is also used for determining the quality of the data products and the sensor.

The determination and evaluation of the performance of optical remote sensing systems is usually done on the basis of fundamental camera parameters. Some of these parameters can change over the lifetime of the sensor and therefore should be checked regularly at specified time intervals after the launch.

In recent years, there have been a variety of activities and publications focused on the geometric and radiometric validation of airborne cameras by EuroSDR (Cramer 2008) and DIN-standards (Reulke et al. 2007).

This paper discusses the characterization of signal-to-noise ratio (SNR) values based on real image data from the RapidEye cameras. The RapidEye camera is a digital pushbroom scanner with 5 spectral bands in the visible and near infrared range. The focal plane was designed by the DLR Institute of Robotics and Mechatronics in Berlin-Adlershof. Each of the 5 detector lines contains 12,000 pixels and sensor elements, respectively. The radiometric dynamic depth of the camera is nominally 12-bit, with A/D conversion of 14-bit. The radiometric calibration for the defined operating point of the cameras is slightly different for the different spectral bands; the corresponding spectral radiance values are between 41 and 88 W/m²/sr/µm. The cameras were built by Jena Optronic in Thuringia. Fig. 1 shows a schematic drawing of the camera structure.

Section 2 presents a short summary of previous papers on the topic of sensor characterization, while in section 3 we explain and discuss our approach. Our results are presented in section 4. In the last section we draw some conclusions.

2 Noise Measurement over Homogeneous and Non-Homogeneous Targets

Let us start by assuming a linear imaging system with a zero-mean white Gaussian random noise that is additive and uncorrelated to the signal. Consider the 2D-problem

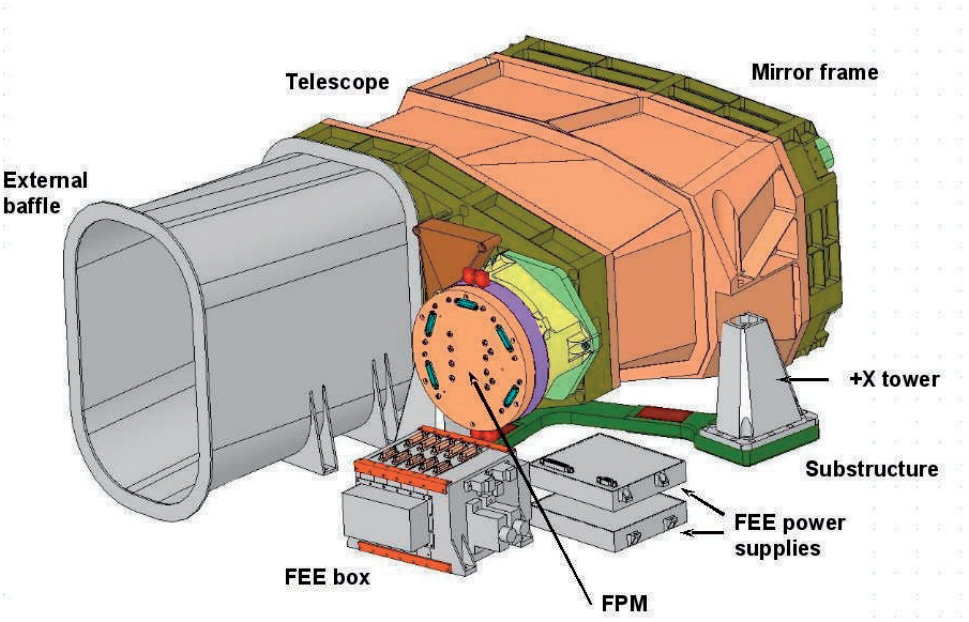

Fig. 1: RapidEye camera architecture and layout (FEE – front end electronic, FPM – focal plane module, +X tower – sensor suspension).

$$y(z_1,z_2) = \iint dz_1' dz_2' H(z_1 - z_1', z_2 - z_2') \cdot x(z_1', z_2') + \xi(z_1,z_2) \quad (1)$$

$H(z_1,z_2)$ is the space invariant point spread function (PSF), $y(z_1,z_2)=y(i\Delta,j\Delta)$ is the sampled measurement (gray) values of the scene $x(z_1',z_2')$ on pixel position $(i\Delta,j\Delta)$ (Δ is the distance between pixels) and ξ the noise of the imaging system. $\xi(z_1,z_2) = \xi(i\Delta,j\Delta)$ are uncorrelated random numbers with zero expectation values:

$$\langle \xi_{i,j} \rangle = 0, \quad \langle \xi_{i,j} \cdot \xi_{k,l} \rangle = \sigma^2 \cdot \delta_{i,k} \cdot \delta_{j,l} \quad (2)$$

The scene can also be supposed to be a stationary random process.

In this paper three different noise components will be taken into account: Dark noise, read noise and shot noise. For an overview about different noise sources in CCD-detectors see e. g. Janesick (2001). The Poisson distributed dark current noise is a parasitic photocurrent in the absence of any illumination on the device, under specified operating conditions (temperature, integration time and bias). Read noise is defined as the temporal system noise of the focal plane assembly (FPA) in darkness. The Poisson distributed shot noise refers to the inherent natural variation of the incident photon flux. Because of the Poisson behaviour, this noise is signal dependent.

An overview about methods for noise estimation is given in Luo & Zhong (2009). The homogeneous area (HA) method estimates the SNR of the image by the ratio of the mean to the standard deviation of manually selected homogeneous areas. The local means and local standard deviations (LMLSD) method automatically estimates the noise by dividing the image into many homogeneous blocks. Other methods for determining the SNR are the residual-scaled local standard deviations (RLSD) method and spectral as well as spatial decorrelation (SSDC) method (Luo & Zhong 2009). For the purposes of our discussion the HA and the LMLSD should be explained more in detail.

The noise determination by the HA method requires an image containing a uniform and homogeneous surface such as a snow field of Greenland or a large homogeneous desert area.

As noise is signal dependent, it has to be determined separately for different signal levels. Unfortunately, most of the homogeneous surfaces mentioned above are very bright and are almost outside the radiometric range for normal operations of the sensor. In addition, systematic noise sources are superimposed to the random noise. Such systematic noise sources could be for instance micro-textures from the observed surface and a not sufficiently corrected PRNU (photo response non-uniformity) in CCD-line direction.

The radiometric characteristics of the sensor have to be determined from periodic measurements over test sites. Both the ground reflectance and the atmosphere are characterized simultaneously and in coincidence with the satellite overpass to estimate the observed at-aperture radiance. An ideal test site for that task should have several critical features (Scott et al. 1996). These include the impact of atmospheric errors (high-reflectance area) and the use of a surface reflectance that should have spatial uniformity (with near-Lambertian reflectance).

In the south-western part of the United States several calibration sites with the above required features exist and have been used for many years. Calibration using these test sites where explained in Pagnutti et al. (2002) and Pagnutti et al. (2011).

The crucial problem with the HA method are the remaining inhomogeneities of the surface. Different approaches have been suggested to overcome this problem of a non-uniform texture of the target.

In the first approach the landscape is considered to be sufficiently uniform to contribute to the low frequency signal. Statistic calculations separate the low frequency contribution to the signal's standard deviation (landscape contribution) from the high frequency contribution to the signal's standard deviation (instrument contribution).

Another method to estimate the SNR consists of selecting homogeneous snowy areas as described in Delvit et al. (2002). As the snow-covered parts of the landscape are nearly uniform, a correct estimation of the noise can be done by calculating the standard deviation of

the signal. As there is little correlation between the noise and the signal from the landscape, images can be decomposed into an image corresponding to the 'pure' landscape and an image of noise.

A completely different approach is the noise-adjusted principal components (NAPC) transform, or maximum noise fraction (MNF) transform (Du & Raksuntorn 2006). The basic idea is to reorganize the data in a way that the principal components are ordered in terms of the SNR, instead of variance as used in the ordinary principal components analysis (PCA). The NAPC transform is very useful in multi-dimensional image analysis. As a result, object information can be better compacted into the first few principal components. A correlation method using bit planes gives reasonable results for decomposition of noise and image texture.

3 Determination of the Noise Equivalent Radiance (NER) from Real Imagery

In this study, the SNR is investigated on the radiance level NER (noise equivalent radiance). Two different methods were investigated. They are based on image data of natural homogeneous and non-homogeneous test areas. The analysis of homogeneous regions is based on a standard method to determine mean and variance of the noise. The second method, used for analyzing inhomogeneous surfaces, searches for homogeneous micro regions (consist of only few pixels) with a homogeneity criterion and clusters the results from these micro regions for NER analysis.

The NER determination with homogeneous targets is based on the evaluation of SNR in manually selected homogeneous areas. Larger homogeneous areas can be found in almost all very bright regions, i. e.. regions with high albedo values. As already mentioned earlier these noise values cannot be compared directly with the system-required values, as those were defined for the lower signal levels of the "normal" operating range, and therefore they are also much lower. To find a way for comparing the measured noise values from bright targets with the system noise requirement, a noise requirement function was derived for each band on the basis of the laboratory calibration. This was done by applying the dependency between the noise value and the signal level to the system noise requirement values determined during the laboratory measurements. If the NER of the measured radiance is lower than the NER derived from the noise requirement function, the requirement is fulfilled. For the interpolation within the range of signal levels used for the calibration this method works quite well. An extrapola-

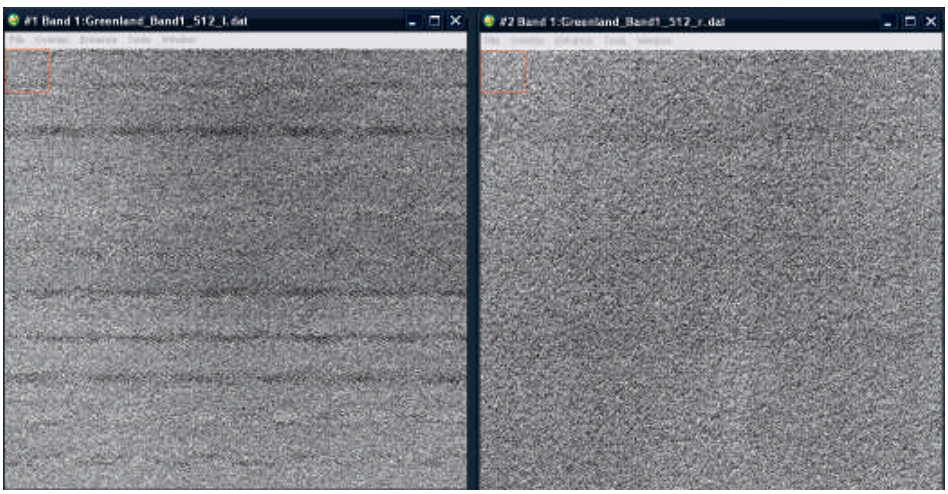

Fig. 2: The Greenland image: Example for systematic noise texture in the left and no systematic noise in the right image.

tion outside of the calibration range with only little uncertainty requires the availability of an accurate photon transfer curve (Janesick 2001).

For the noise determination homogeneous regions in the images were preselected manually. Subsets of 1024 × 1024 pixels were cut out in the central image part. These homogeneous image patches where extracted based on predefined criteria (related to the texture) and were used to evaluated the NER.

The selection procedure for homogeneous areas can be described as follows. In most cases, objects with a reflectivity of about 5 % to 20 % are investigated. In this reflectivity range areas with a homogeneous surface are normally very small and randomly distributed over the image. Therefore, splitting the image into many homogeneous blocks seems insufficient and additional procedures are required to recognize and analyse smaller homogeneous areas.

As already mentioned, the signal noise depends on the signal level. Moreover, for each image, random and systematic noise components are superimposed and sum up to a combined noise level. Systematic noise sources (e. g. micro-texture from the observed surface, not sufficiently corrected PRNU) can be superimposed to the random noise coming from the sensor. As an example an image part containing some remaining systematic noise is shown in Fig. 2 (left side). Images with this kind of noise are excluded for further investigation.

The image shown in Fig. 2 is not a typical example for the type of images we tried to analyse here, but we will use it later on for tests and comparison purposes. A more adequate image example is shown in Fig. 3.

For this more realistic type of images an automated procedure was developed to extract small homogeneous areas from the generally inhomogeneous image parts. Within these small areas it was assumed that the surface texture is negligible. The mean and standard deviation of the signal can be computed for these small areas. An advantage of this method is that it automatically measures noise values at different signal levels because of the different reflectance of the extracted small homogeneous image areas.

The procedure is formally based on the "homogeneous area" method used by Gao (1993) which was extended by Gao et al. (2008). For each image pixel texture information was derived in blocks around the pixel, with block sizes of 3 × 3, 5 × 5, …, 11 × 11 pixels. The ho-

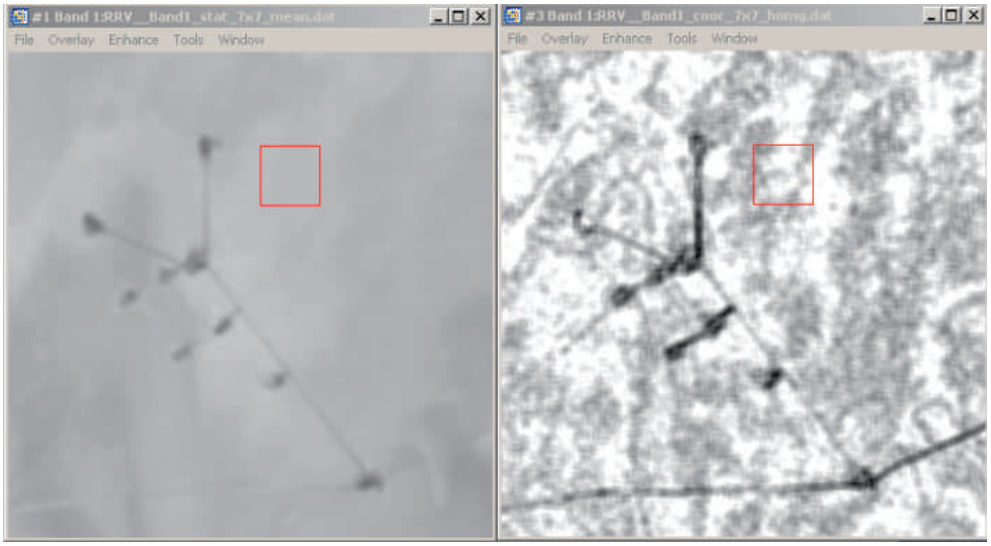

Fig. 3: Original image and homogeneity measure (right) for this image part. The image is from Railroad Valley Playa in Nevada. The left image seems homogenous except for the roads. The calculated homogeneity is seen in the right part, where bright regions stand for high homogeneity.

mogeneity texture measures were applied to the data in these blocks. In addition the mean and the standard deviation of the gray values were computed. The first step is to extract blocks with a sufficient homogeneity. It turned out that the parameter "homogeneity" derived from the *Gray-Tone Spatial-Dependence Matrix* or *Gray Level Co-Occurrence Matrix* (GLCM) (Haralick et al. 1973) is suitable for the determination of the homogeneity level $h_{i,j}$ (inverse difference moment) at pixel (i,j):

$$h_{i,j} = \sum_{k=1}^{N} \sum_{l=1}^{N} \frac{c_d(k,l)}{1+(k-l)^2} \qquad (3)$$

In eq. 3, $c_d(k,l)$ is the GLCM, a statistical measure that contains information about the positions of pixels having similar gray level values, but does not provide any information about the repeating nature of texture. Furthermore, $d = (m \cdot \Delta, \cdot n \cdot \Delta)$ is a displacement vector. The GLCM counts all pairs of pixels separated by (m, n) pixels having the gray levels k and l. The matrix c_d has the size (N,N); N is the number of quantized gray levels. In a homogeneous image patch the range of gray levels is small and c_d will be clustered near the main diagonal. The denominator $1 + (k–l)^2$ enhances this trend. A heterogeneous image patch will be more spread. The GLCM can be calculated in different direction s (with respect to neighbouring pixel) and distances d (in pixels).

The image shown in Fig. 3 (left) is taken from Railroad Valley Playa in Nevada. The local homogeneity (right) is a measure for local similarity in the image. To achieve a separation between noise and texture, only the regions or small areas with the greatest homogeneity were used for the further evaluation.

Considering the LMLSD method only pixels with sufficiently high homogeneity (close to 1) are involved in a data clustering process. For each cluster, which is related to a mean measured radiance, the variance-histogram is analyzed. It is assumed that the variance relative to the maximum of the histogram is representative for the measured radiance.

In a first test this approach is applied to the Greenland scene (Fig. 2, right) and the HA and LMLSD method are compared. Here a homogeneous area with almost only random noise will be assumed. The approach described above can therefore be directly compared to the SNR determination from the whole image part. The idea behind this is to check whether the results, i. e.. the calculated noise, according to the new method are comparable to the noise determined in the "classical" HA method. Fig. 4 shows the variance distribution and the overall result. The calculated mean is equal for both methods; the local variance deviation is related to the maximum for this data set (see Fig. 4, left) but is about 5 % - 10 % lower then the variance derived from the entire image.

To apply this procedure to an image with a complex surface texture (Fig. 3) some additional effort is required for the interpretation of the results. Fig. 5 shows the local variance with respect to the local mean for parts with maximum homogeneity. The threshold for the homogeneity value was set to 0.98.

Obviously this procedure generates a large number of small image segments with homogeneous radiometric behaviour. Regions where the image brightness changes strongly

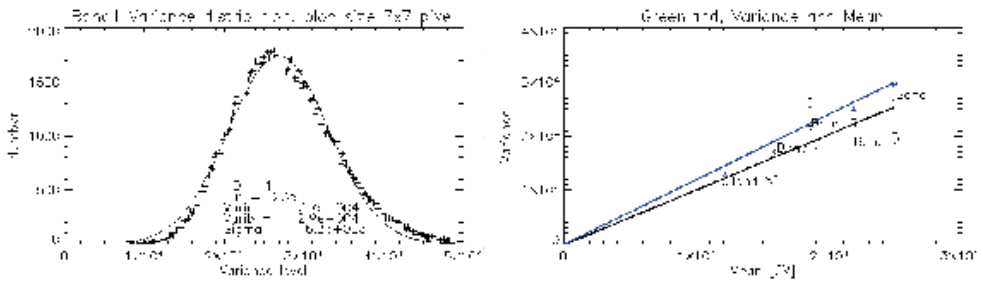

Fig 4: Variance distribution derived from LMLSD method with a maximum near the variance of the whole data set (left) for the Greenland image. Variance over mean dependence for all bands (black) with confidence interval (right) and variance derived with HA method (blue).

are excluded automatically in this procedure. As seen in Fig. 5 (left), for the extracted image parts with maximum homogeneity a data clustering with respect to the local mean seems to be possible. This was done here with histogram analysis (see Fig. 5 (right)). This procedure is equivalent to a classification based on texture parameters. The clustering however is only possible if the segmentation leads to patches that are homogeneously better than a predefined threshold value.

Fig. 6 presents the histogram of the local variance for a certain cluster. Between the minimum and the maximum of the local variance (lv), a fixed number of variance values with equal width (bins) are combined. In other words, the histogram is coarsened.

Furthermore the influence of the image block size was investigated. Four different block sizes (5×5, 7×7, 9×9, 11×11) where used for this investigation. The results show a significant influence of the block size. With increasing block size the segmentation between clusters becomes better. At the same time the number of blocks which fulfil the homogeneity criteria becomes smaller. As an optimal trade-off between these two parameters a block size of 7×7 was used in the following investigations.

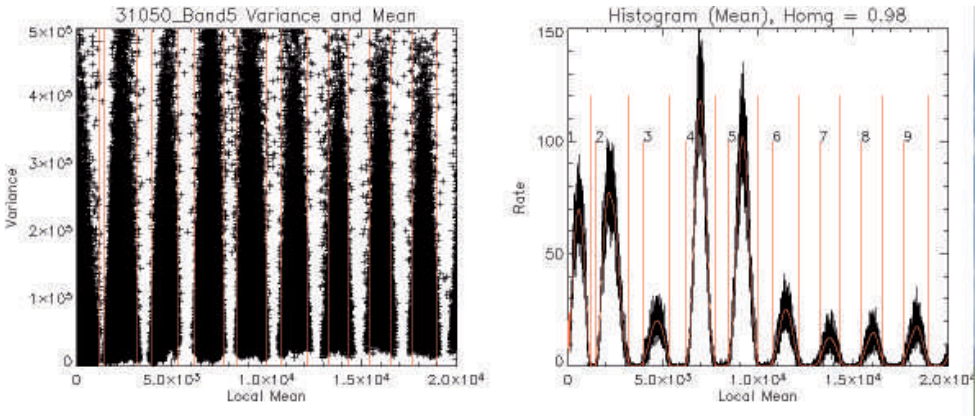

Fig 5: Selected groups in the local mean – variance plot (left). Local mean histogram (right) is derived from data in the left plot and shows the selection of different clusters (related to the numbers).

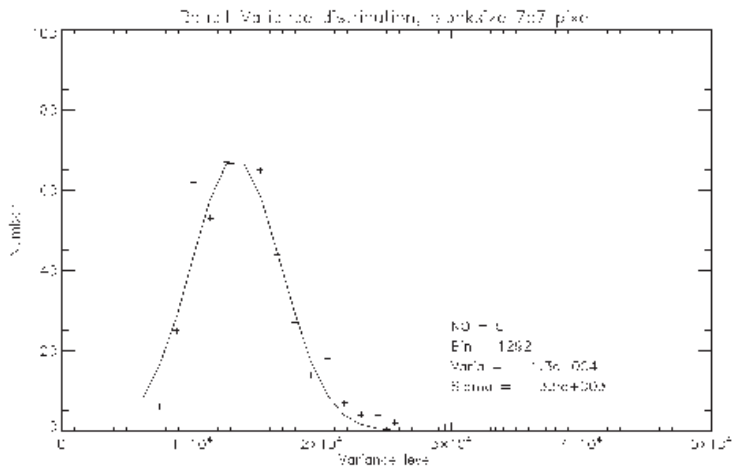

Fig. 6: Histogram of the local variance (example).

4 Results and Discussion

Fig. 7 shows the result for the NER in relation to the radiance for Band 1. For the defined system reference radiance the measured NER can be derived from the blue fitting line. Due to the Poisson distributed photon noise, the NER increases with the measured radiance.

Based on this method an in-flight determination of the radiometric image noise is possible. By comparison of the in-flight noise determination results with the NER values defined as system requirements it is possible to check whether the system is still within the specifications.

As an example, Fig. 8 shows the results for the Blue- and the Red-Edge bands of the RapidEye camera. The black diamonds in the Fig. 8 represent the in-flight calibration noise values, whereas the dotted colour lines show the pre-flight laboratory noise measurements for all five RapidEye sensors. The vertical black lines through the diamonds indicate the confidence intervals derived from the in-flight calibration measurements. The single blue star represents the system noise requirement for the RapidEye cameras, which e. g. for the Blue Band was defined at a radiance level of 72 W/m²/sr/µm. The two examples show clearly that using the presented in-flight noise determination method, a significant part of the radiometric range for normal camera operations could be covered although it was impossible to get data of the full radiometric range compared to the laboratory calibration measurements.

It is also obvious that the results of the in-flight noise measurements are in good agreement with the pre-flight calibration values for the camera noise. This is a strong indication that the camera systems are still working according to the RapidEye system specifications. No significant change of the camera characteristics regarding sensor noise after the launch and during normal operational work could be observed up to now. The measured values are clearly below the system noise requirements for the RapidEye sensors.

5 Conclusions and Outlook

The procedure described in this paper allows the evaluation of image noise directly from operational image data after the launch of a satellite sensor. This method is very important for the after-launch monitoring of the sensor quality and health status of the sensor by comparing periodic noise measurement results with the initial values defined by the system requirements.

The major problem for noise determination was to eliminate the impact of remaining sur-

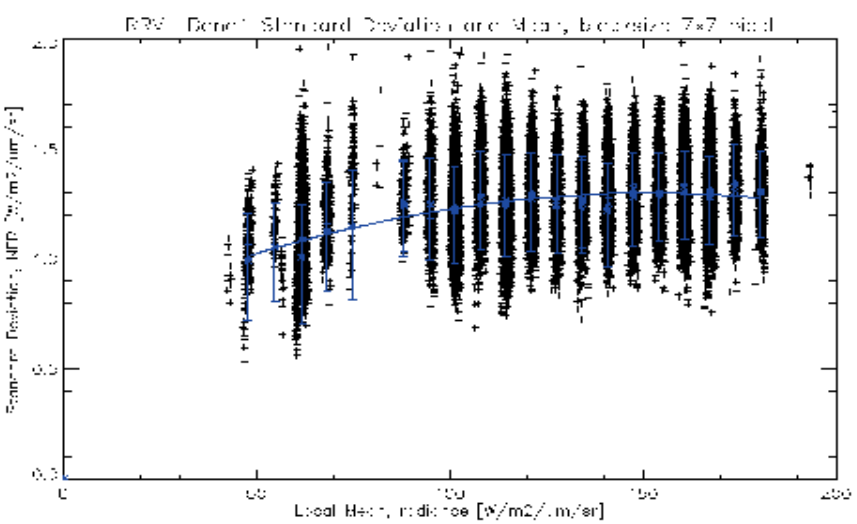

Fig. 7: Radiance vs. noise equivalent radiance (Band 1).

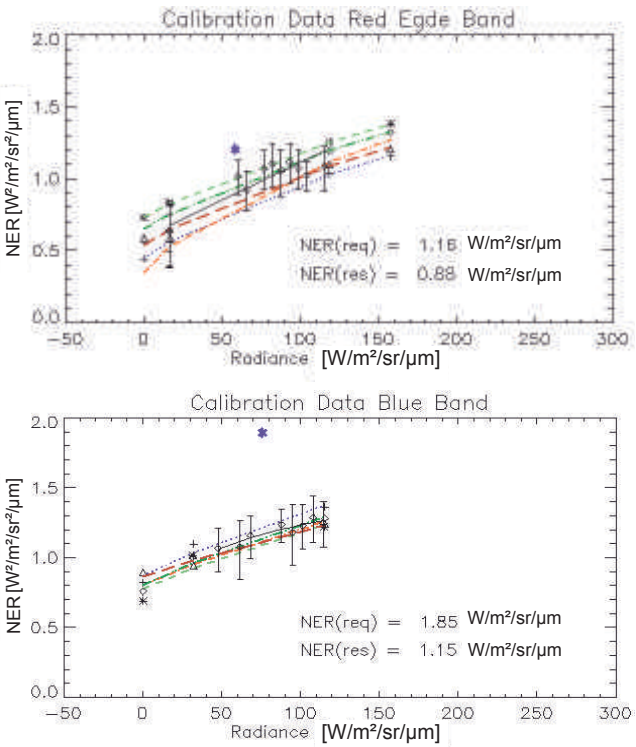

Fig. 8: Comparison of the pre-flight lab noise calibration and the in-flight noise determination according to the described procedure – Blue Band (below) and Red-Edge Band (above).

face structure. In contrast to Gao (1993), for each pixel, the local mean and variance are be determined within a block of predefined size around each pixel. To determine the influence of the remaining microstructure of the surface, an additional homogeneity criterion was used.

It was shown that with the proposed method an improvement of the NER determination for typical albedo values could be achieved. The procedure has been implemented as a semi-automatic scripted work flow. Based on this method, all 5 bands of all RapidEye cameras have been analysed. Exemplary results with two bands were presented in section 4.

In our future work, these results have to be double-checked with data from other sensors. In particular, the homogeneity criteria can be replaced by other criteria, e. g. the one described in Brügelmann & Förstner (1992).

Acknowledgements

We would like to thank Mr. Scott Douglas for the review of the article with respect to content and language.

References

Brügelmann, R. & Förstner, W., 1992: Noise Estimation for Color Edge Extraction. – In: Förstner, W. & Winter, S. (eds.): Robust Computer Vision. – Karlsruhe **1992:** 90–107.

Cramer, M., 2008: The EuroSDR approach on digital airborne camera calibration and certification. – ISPRS Congress Beijing, IAPRS, Volume **XXXVII** (B4): 1753–1758.

Delvit, J.-M., Leger, D., Roques, S., Valorge, C. & Viallefont-Robinet, F., 2002: Signal-to-noise ratio assessment from nonspecific views. – In: Serpico, S.B. (ed.): Image and Sig-

nal Processing for Remote Sensing VII **4541:** 370–381.

Du, Q. & Raksuntorn, N., 2006: Hyperspectral image analysis using noise-adjusted principal component transform. – In: Shen, S.S. & Lewis, P.E. (eds.): Algorithms and Technologies for Multispectral, Hyperspectral, and Ultraspectral Imagery XII **6233**.

Haralick, R.M., Shanmugam, K. & Dinstein, I.H., 1973: Textural Features for Image Classification. – Systems, Man and Cybernetics, IEEE Transactions on **3** (6): 610–621.

Gao, B.-C., 1993: An operational method for estimating signal to noise ratios from data acquired with imaging spectrometers. – Remote Sensing of Environment **43** (1): 23–33.

Gao, L.R., Zhang, B., Zhang, X., Zhang, W.J. & Tong, Q.X., 2008: A new operational method for estimating noise in hyperspectral images. – IEEE Geoscience and Remote Sensing Letters **5** (1): 83–87.

Luo, W. & Zhong, L., 2009: The effect of spatial resolution on the noise estimation in hyperspectral images. – In: Udupa, J.K. et al. (eds.): Multispectral Image Acquisition and Processing. – SPIE **7494**.

Janesick, J.R., 2001: Scientific charge-coupled devices. – 920, SPIE Press **PM83**.

Pagnutti, M., Holekamp, K., Ryan, R., Blonski, S., Sellers, R., Davis, B. & Zanoni, V., 2002: Measurement sets and sites commonly used for characterizations. – Proceedings of the ISPRS Commission I Mid-Term Symposium 2002: Integrated Remote Sensing at the Global, Regional and Local Scale **XXXIV**.

Pagnutti, M., Ryan, R., Blonski, S., Holekamp, K., Cramer, M., Helder, D. & Honkavaara, E., 2011: Targets, methods, and sites for assessing the in-flight spatial resolution of electro-optical data products. – Canadian Journal of Remote Sensing, Published on the web 12 May **2011**.

Reulke, R., Dörstel, C. & Schwebel, R., 2007: DIN 18740 "Photogrammetrische Produkte" Teil 4: Anforderungen an digitale Luftbildkameras und digitale Luftbilder. – DGPF Jahrestagung **2007:** 281–286.

Scott, K.P., Thome, K.J. & Brownlee, M.R., 1996: Evaluation of the Railroad Valley playa for use in vicarious calibration. – Proceedings of SPIE **2818:** 158–166.

Addresses of the Authors:

Prof. Dr. Ralf Reulke, Humboldt-Universität zu Berlin, Institut für Informatik, Computer Vision, Unter den Linden 6, 10099 Berlin, Germany, e-mail: reulke@informatik.hu-berlin.de

Dr. Horst Weichelt, RapidEye AG, Molkenmarkt 30, 14776 Brandenburg an der Havel, Germany, e-mail: weichelt@rapideye.de

Manuskript eingereicht: Mai 2011
Angenommen: November 2011